VI Serbian-Belarusian Symp. on Phys. and Diagn. of Lab. &
Astrophys. Plasma, Belgrade, Serbia, 22 - 25 August 2006
eds. M. Ćuk, M.S. Dimitrijević, J. Purić, N. Milovanović
Publ. Astron. Obs. Belgrade No. 82 (2007), 183-200 *Invited lecture*

EXCESSIVE DOPPLER BROADENING OF H_α AND D_α LINE IN A HOLLOW CATHODE GLOW DISCHARGE

N. M. Šišović[1], G. Lj. Majstorović[2], N. Konjević[1]

[1] *Faculty of Physics, University of Belgrade, 11001 Belgrade, P.O. Box 368, Serbia*
[2] *Military Academy, 11105 Belgrade, Pavla Jurišića – Šturma 33, Serbia*

Abstract. A review of experiments dealing with excessive Doppler broadening (EDB) of hydrogen and deuterium Balmer lines in hollow cathode gas discharge(s) is presented. The experimental data of excessive line broadening are discussed from the point of view of the sheath-collision model and the resonance transfer model. The results of new experiments reported here indicate that EDB part of hydrogen Balmer lines may be used for discharge-cathode surface interaction monitoring.

1. INTRODUCTION

Since the discovery of excessive Doppler broadening of hydrogen Balmer lines [1,2], experimental studies, see e.g. Refs. 3-4, have been conducted to resolve and understand processes related to this phenomena. The shape of these lines emitted from some low-pressure gas discharges operated with hydrogen isotopes or hydrogen gas mixtures with inert gases exhibits unusual multi component behavior, see e.g. Figures 1a-4a. The same EDB shapes of H_α and H_β lines are detected in a plane cathode glow discharge operated with various gas mixtures with hydrogen [5].

The origin of the narrowest part of the profile in Figure 1a is related to the Doppler broadening of the thermalized excited hydrogen atoms H^* in the negative glow region of the discharge. The broader middle part of the line profile is related to excited hydrogen atoms generated in electron collisions with H_2. The pedestal of the line profile is very broad indicating that energetic excited hydrogen atoms having energies larger than hundreds of electron volts are generated in (the) discharge. The presence of large energy excited hydrogen atoms implies that fast hydrogen atoms H_f of higher energy exist in the discharge [6]. As pointed out already, the origin of the narrow- and medium-width part of the line profile may be explained on the basis of well-established processes.

The primary explanation of the broadest part - pedestal of the line profile comes from the sheath-collision model. In this model ions H^+ and H_3^+ are accelerated in a high-voltage discharge sheath and produce fast H atoms in charge transfer/dissociation collisions with the matrix gas–molecular hydrogen. The fast H atoms are then excited and scattered in another collision. The same excitation process is occurring with H atoms backscattered from the cathode [3,7,8]. In the Ar-H_2 discharge, see the H_α profile in Figure 1b, the contribution of H^+ ion is negligible in comparison with that of H_3^+ ion, see e.g. [6,9]. The latter ions fragment in collisions with matrix gas or at the cathode surface generating H_f atoms of lower energy, and consequently lower energy excited atoms H^* are produced. For EDB in DC discharges see [1-13].

Another model of EDB has been proposed by Mills *et al.*, see e.g. [14,15]. According to this model, in the resonance transfer (RT) process H atoms react with certain ions, for instance He^+, Ar^+ or other "resonance catalysts" produced by the electric discharge, to generate excess energy. The RT process is followed by excessive Doppler broadening of the hydrogen Balmer lines, which according to references [14,15] reveals the presence of high energy excited hydrogen atoms-carriers of excess energy produced in the RT process.

In this paper a review of publications dealing with the excessive Doppler broadening hydrogen and deuterium Balmer lines in hollow cathode gas discharge will be presented and discussed from the point of view of both models, when it is possible. Also, it will be demonstrated that some new results dealing with this subject may be used for discharge-cathode surface interaction monitoring [16].

2. THE INFLUENCE OF CATHODE MATERIAL, GAS COMPOSITION AND ELECTRIC FIELD DIRECTION ON EDB IN HOLLOW CATHODE DISCHARGE

In the recent paper [15] the authors of RTM reported study of the excessive H_α broadening in various discharges including hollow cathode discharge. The results in Table I [15] and discussion firmly state that excessive broadening is detected only in Ar and He mixtures with hydrogen while in H_2, and in mixtures Ne-H_2 and Xe-H_2 no effect is found. This result is expected on bases of their RTM. The aim of a recent experiment [13] in our laboratory is to test these results.

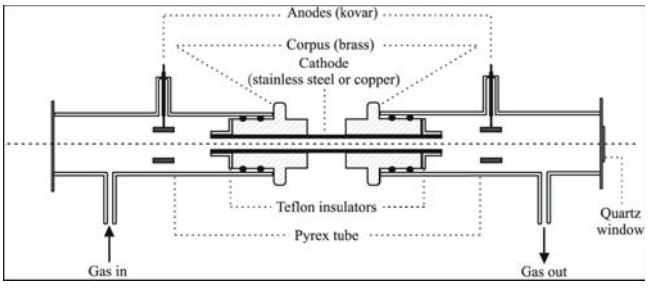

Fig 1. The hollow cathode discharge tube [13].

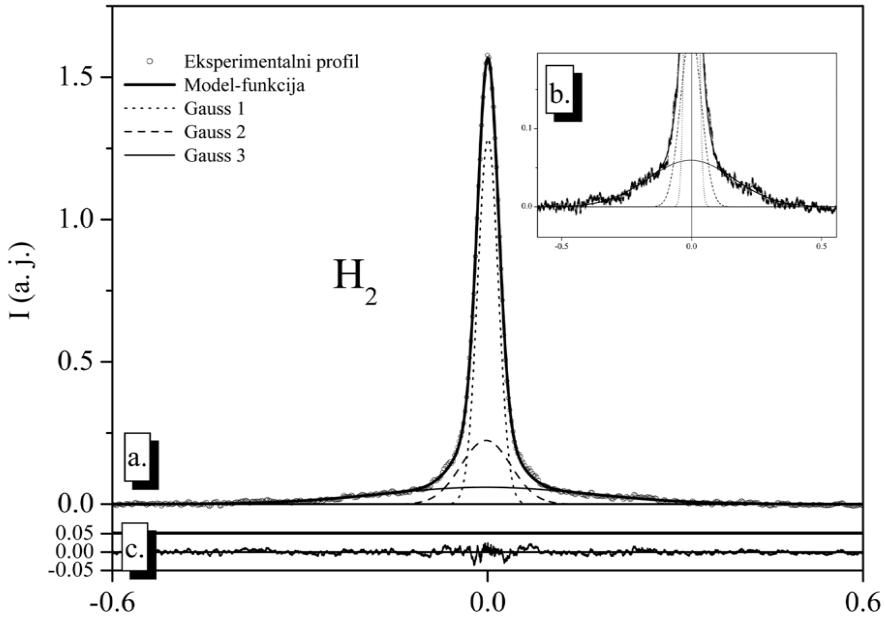
Eksperimentalni profil
Model-funkcija
Gauss 1
Gauss 2
Gauss 3
H2
I (a. j.)
a.
b.
c.
1.5
1.0
0.5
0.0
0.05
0.00
-0.05
-0.6
0.0
0.6

A

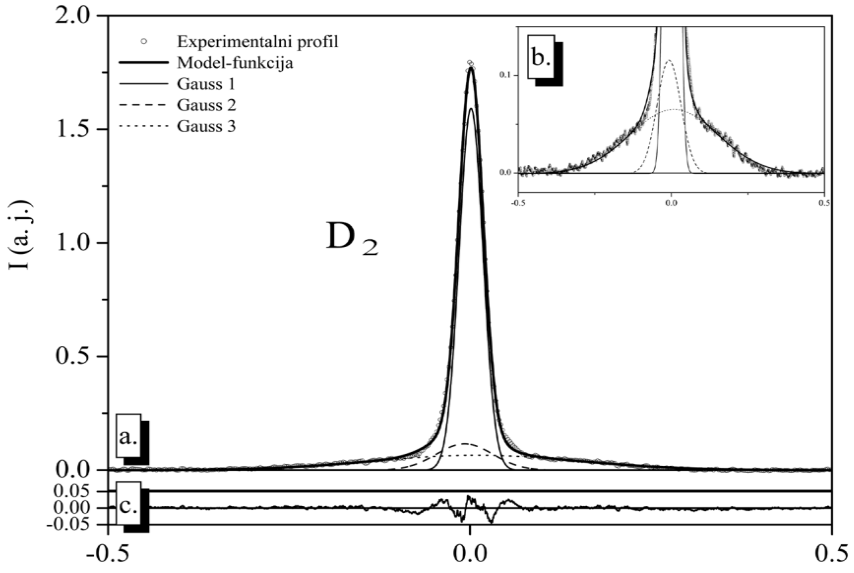
Experimentalni profil
Model-funkcija
Gauss 1
Gauss 2
Gauss 3
D2
I (a. j.)
a.
b.
c.
2.0
1.5
1.0
0.5
0.0
0.05
0.00
-0.05
-0.5
0.0
0.5

B

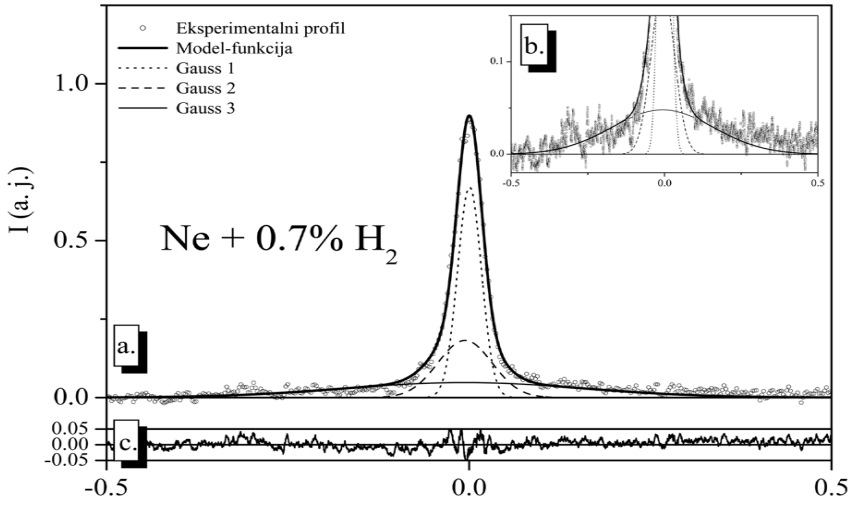

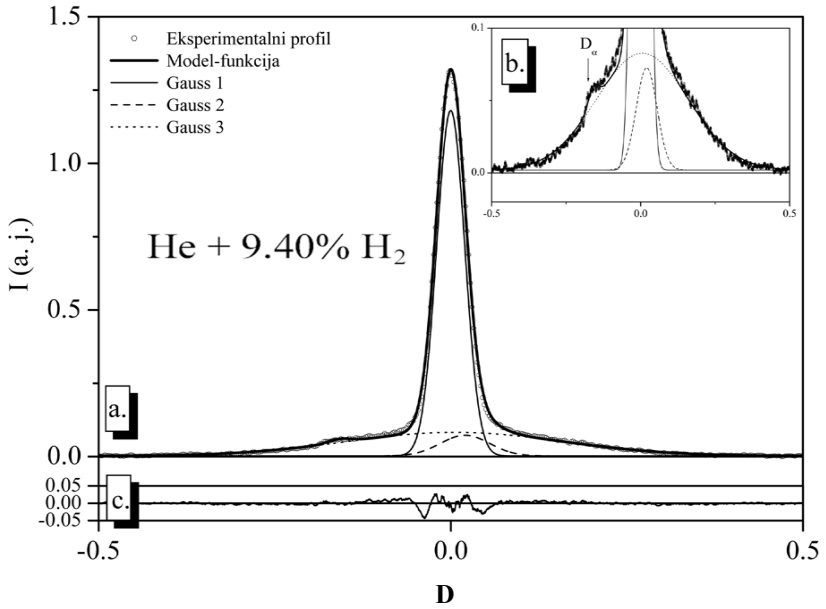

Fig. 2. Typical H_α line shapes recorded end-on from high pressure low-voltage copper hollow cathode glow discharge and fitted with three Gaussians: (a) H_α line shape, (b) the enlarged part of H_α line shape excessively broadened; and (c) the residual plot. **A.** Discharge conditions: pure hydrogen; front anode, p=2mbar, U=440V, I=90mA. **B.** Discharge conditions: pure deuterium; front anode, p=2mbar, U=490V, I=90mA. **C.** Ne-H_2 mixture (99.3%:0.7%); front anode, p=2mbar, U=250V, I=90mA. **D.** He-H_2 mixture (90.6%:9.4%); front anode, p=2mbar, U=323V, I=90mA. [13]

Newly developed hollow cathode glow discharge with stainless steel or with copper cathode is used, see Fig.1. The construction details follow basic concept of pyrex-kovar design reported in [17]. Both cathodes were 100 mm long with 6 mm internal diameter. Kovar anodes, 5 mm long with 15 mm dia, are located at the both ends of cathode at a distance of 15mm.

Typical examples of the H_α line shape recordings from the central region of copper hollow cathode high pressure low-voltage glow discharge are given in Fig. 2. Three components can be distinguished in the overall fit of the symmetric H_α and D_α line shapes in pure gases and gas mixtures, see Fig. 2: central narrow peak, broader middle part and far drawn-out pedestal. The overall fit involving convolution of three Gaussians in Fig. 2 may be justified in two ways: *(i)* three groups of excited hydrogen atoms are expected in the negative glow region: thermalized H^* typical for negative glow (Gauss 1); a group of H^* atoms produced by dissociation of H_2 molecules in collisions with high energy electrons (Gauss 2); and a group of H_f^* atoms generated in collisions of H_f reflected from the cathode with H_2 (Gauss 3) and *(ii)* a good quality of three gaussian fit, see the residue plot in Fig. 2.

The examples in Fig. 2 show that the excessive H_α or D_α line broadening is present in both hollow cathodes discharges under all studied experimental conditions. Furthermore, there is nothing exceptional about discharge operating in He-H_2 mixture, where, according to RTM, resonance transfer catalysts He^+ are present: the profiles, recorded from our discharges operating in He-H_2 mixtures, have a typical multipart component structure in contrast to a single excessive broadened profile recorded in the same gas mixture and reported in [15].

On the basis of earlier experiment, see Fig.9 in [3], high D_f^* temperatures are expected and they are detected in both hollow cathode discharges. The presence of high energetic neutrals D_f^* in this case is related to large back scattering coefficients of D^+ from the cathode surface, which exceeds ~50% same coefficients of H^+ [18]. These ions are neutralized at the cathode and reflected back in the form of D_f, which collide with matrix gas D_2 and produce observed D_f^* [2]. High voltage in deuterium discharge plays an important role in D^+ acceleration and in this way to generation of high temperature D_f^*.

The comparison of data obtained for different cathodes shows also that Gauss 3 contribution to the overall profile is significantly larger in case of copper than stainless steel hollow cathode discharge. This result is in qualitative agreement with results from PCGD discharge, see Fig.7 in [3,4] and may be explained by larger back scattering coefficients of H^+ from Cu surface in comparison with Fe [3,4,18]. It proves that the concentrations and energies of H_f^* depends of cathode material and that, most likely, is associated with sputtering yield and characteristic back-scattering coefficients [4].

As pointed out already in Introduction, the electric field is essential for the CM to explain basic processes related to excessive Doppler broadening. The only fact in this experiment that looks in favor of RTM: the H_α line shape measurements are performed primarily by observing the negative glow region of discharge where large electric fields do not exist. Since the excessive broadening is detected in this region one may conclude that this proves validity of RTM. However, one should also bear in mind that accelerated H^+ and H_3^+ ions in a cathode fall region of

discharge operated at high pressure and low-voltage regime are back-scattered towards the center of hollow cathode in the form of fast hydrogen atoms, which generate H_f^* in collisions with matrix gas. Thus, the presence of observed excess Doppler H_α broadening, Gauss 3, may be well explained within CM.

In order to examine further the importance of electric field for excessive Doppler broadening an experiment with stainless steel hollow cathode glow discharge in a low pressure, high-voltage regime is carried out. This is the case when electric field vector is coaxial with hollow cathode axis and its direction may be changed by applying rear or front anode, see Fig. 3.

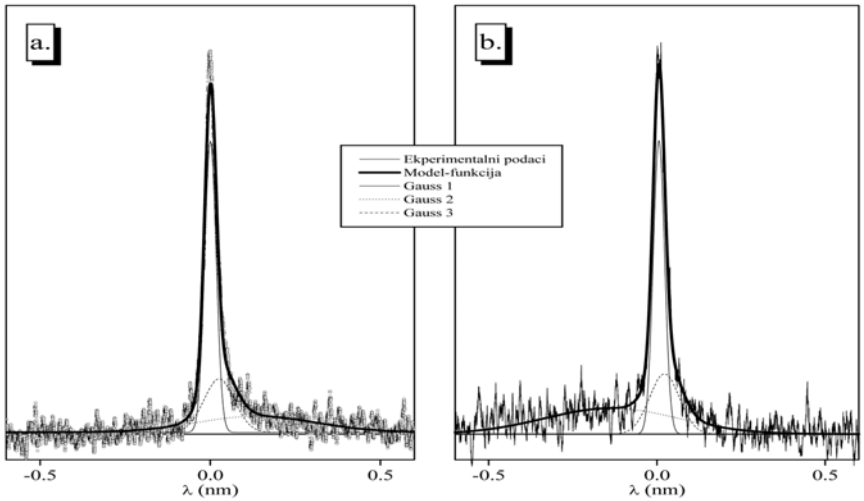

Fig. 3. Typical H_α line shapes recorded end-on from low pressure high-voltage discharge (He-H_2) mixture; stainless steel cathode) and fitted with three gaussians: **(a)** front anode and **(b)** rear anode. Discharge conditions: p=1mbar, U=1030V, I≈5mA. [13]

The results in Fig. 3 clearly show that Gauss 3 may be shifted into blue or red wavelength direction by simply changing the direction of electric field vector. Similar experiment with hollow cathode glow discharge operated with higher voltages in pure hydrogen is reported in [17,19]. The dependence of shift direction of high temperature component upon electric field vector is the same as in Fig. 3. Both experiments, [17] and this one, undoubtedly prove the importance of electric field for the excess Doppler broadening. The RTM in contrast to CM does not depend upon electric field and can't be used to explain results in Fig. 3.

Moreover, Phelps [20,21] reported recently a thorough comparative analysis of Mills and co-workers RT experiments and most of the other EDB Balmer line studies. On the bases of this analysis and the fact that Mills and co-workers [14,15] do not provide a set of elementary processes with cross sections for converting the energy of RT products into the fast excited hydrogen atoms, one may conclude that RT model cannot be used to explain EDB of hydrogen Balmer lines.

On the other hand, a number of experiments disagree with RT model predictions, see e.g. [20,21] and references therein. Therefore, the sheath-collision model will be used from this point forward for the interpretation of EDB results.

3. EXCESSIVE BROADENING OF HYDROGEN BALMER LINES FOR DISCHARGE-SURFACE INTERACTION MONITORING

Several experiments [10,11], in particular the recent ones [6,9,13] carried out with measurements perpendicular to the electric field, showed symmetric line profiles, which can be precisely analyzed. The possibility of separating the EBD part of the H_α profile has enabled determination of cross section data for $H \rightarrow H_2$ collisions in an abnormal glow discharge [6]. Also, it has been demonstrated that the EDB part of hydrogen Balmer lines may be used for discharge-cathode surface interaction monitoring [16].

In this experiment, the H_α line shape and the effective sputtering rates were monitored using intensities of Ti or Fe, Ni, and Cr resonance lines in a hollow cathode (HC) discharge operated using H_2 or (a) the Ar-H_2 mixture at a pressure of 2 mbar. For comparison with the Ar-H_2 experiment, all relevant measurements are also carried out in an Ar discharge. During the discharge operation, cathodes were either air cooled or gradually heated by switching off the fan. The temperature of the outer wall of the HC tube is measured by a K-type thermocouple.

Three components of the line profile are determined by fitting the H_α line with three Gaussians, see Figs. 4 and 5. Due to low sputtering yield of hydrogen ions, observations of resonance lines are performed in Ar–H_2 and Ar only. Line intensities were measured at different electrical power inputs induced by a change of discharge voltage at constant current, see Figs. 6(c) and 7(c). Line intensities normalized to the unit electrical power input are given in Figs. 6(a) and 7(a).

Titanium. Figure 6 shows for H_2 and Ar–H_2 discharges, a gradual increase of G_3/G_{total} with temperature, where G_i (i=1,2,3) is the area of the corresponding line component. This is in agreement with earlier results, showing that implanted hydrogen in Ti lowers the reflection of H after bombardment with protons [22]. Experimentally, it is determined that the H particle reflection coefficients R_N of TiH_2 is less than 30% lower than for Ti [23], while simulations predicted 50% [24]. During an increase of cathode temperature, a lowering of the TiH_2 concentration is expected and consequently G_3 increases. At elevated temperatures (>230^0C), not reached in this experiment, no hydride contribution is expected [25]. Figure 6(b) supports an assumption of the TiH_2 influence to the G_3 contribution. The intensity of Ti I resonance lines at lower temperatures in Ar–H_2 discharges are smaller than in Ar discharges in spite of energetic ArH^+ ions present in the mixtured-species discharge [26]. At higher temperatures, Ti line intensities in the Ar–H_2 case gradually overcome those in Ar as a consequence of the lowering H/Ti ratio.

Stainless steel. Similar to the Ti surface case, the G_3 contribution in H_2 discharge increases with temperature, see Fig. 7(b), and may be related to an increase of SS reflectivity with decreasing H/Fe ratio [24]. The large and almost constant G_3 in Ar–H_2 is explained by: *i)* a large presence of H_3^+ ions; and *ii*) negligible influence of iron hydrides at the SS surface under the influence of

energetic ArH^+ sputtering. Generally, hydrogen in the SS matrix may be characterized by fast diffusion and reemission leading to a smaller surface concentration [22]. Consequently, in contrast with the Ti case, see Fig. 6(a), Fe, Cr and Ni resonance lines in Ar-H_2 are always larger intensity than in the Ar discharge, see Fig. 7(a). From the sputtering point of view, SS is considered to behave as a single-component system [27]. Ratios of line intensities in Fig. 7(a) show, at lower cathode temperatures, good agreement with values expected from SS composition. At higher cathode temperatures when sputtering yield increases, the intensity of Fe resonance line shows slower increase due to the self-absorption effect.

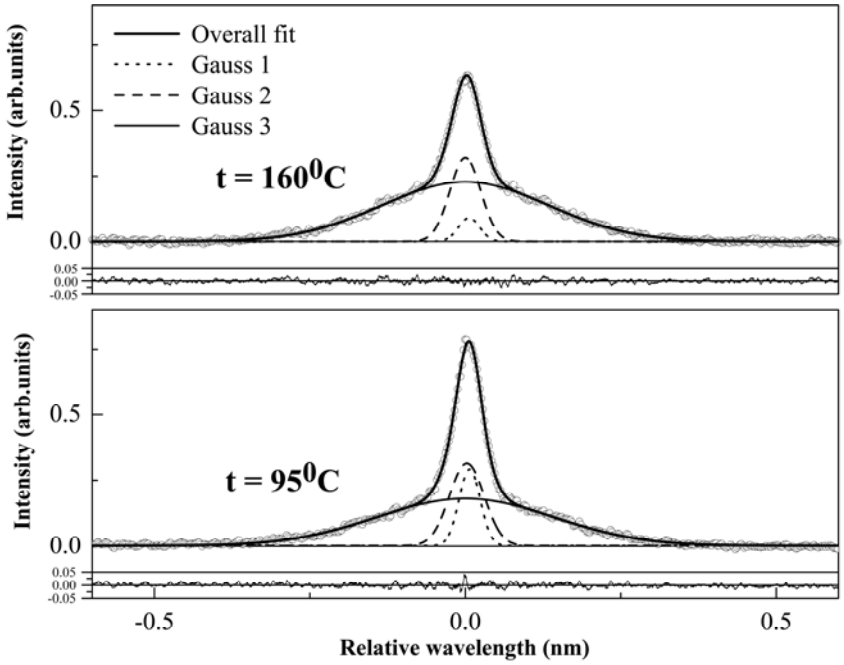

Fig. 4. The H_α line profiles recorded along the axis of titanium hollow cathode glow discharge in Ar–H_2 fitted with three Gaussians. Discharge conditions: I=90 mA and p=2 mbar [16].

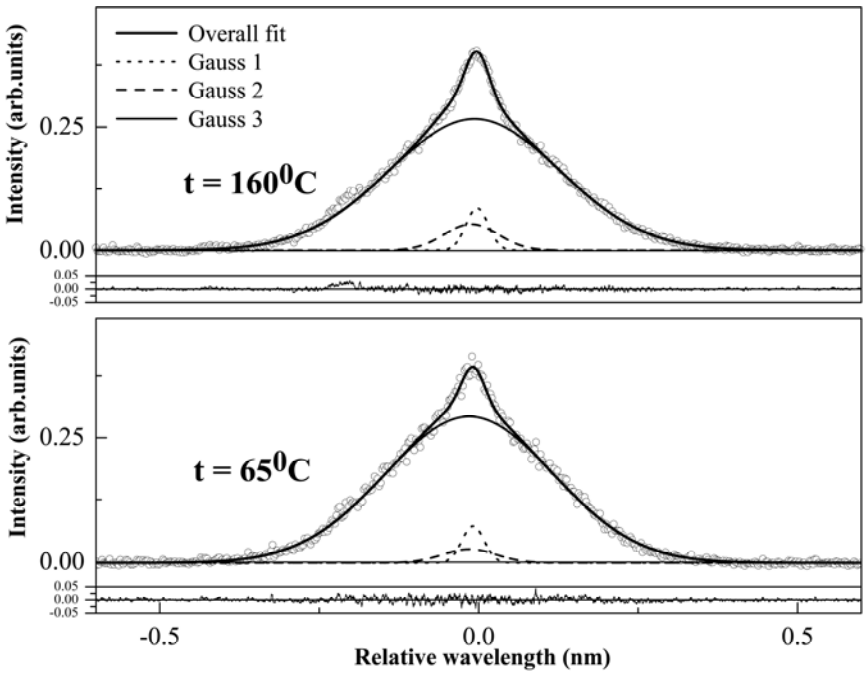

Fig. 5. The H_α line profiles recorded along the axis of stainless steel hollow cathode glow discharge in Ar–H_2 fitted with three Gaussians. Discharge conditions: I=90 mA and p=2 mbar [16].

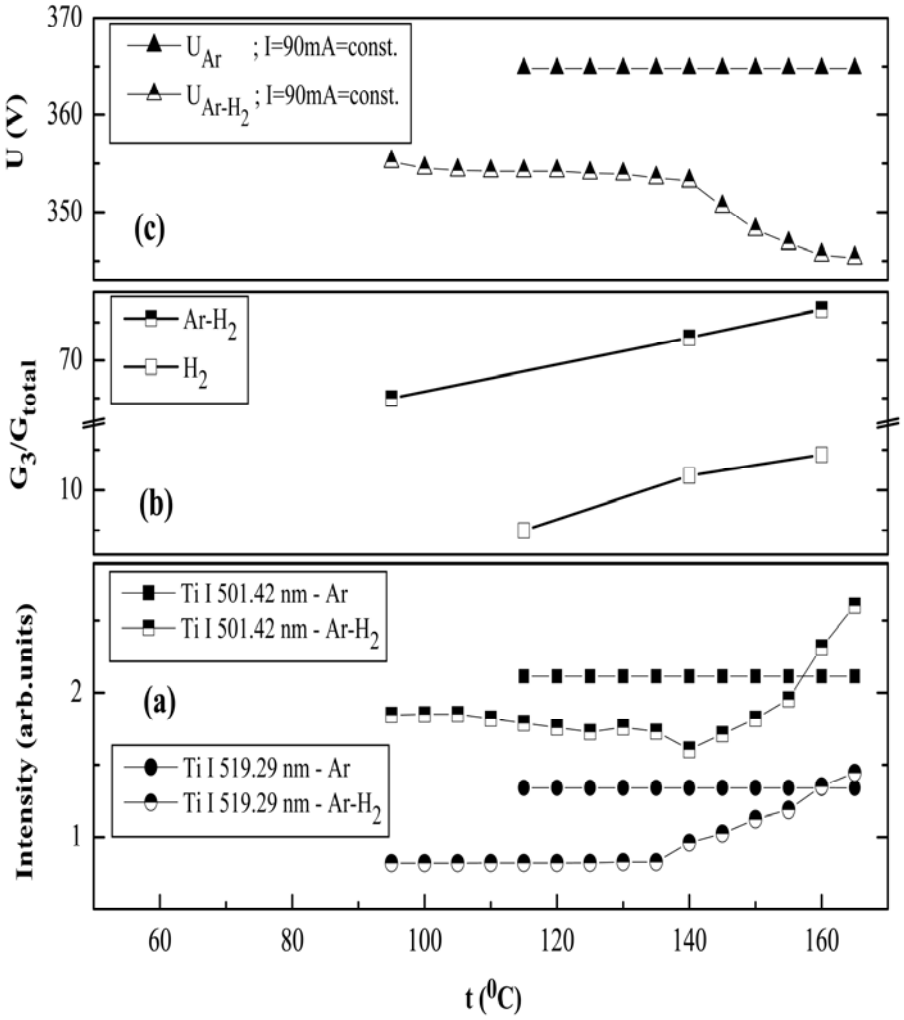

Fig. 6. The temperature dependence of: (a) Ti resonance lines intensity; (b) contribution of G_3/G_{total} to the H_α profile in H_2 and in Ar–H_2 ; and (c) discharge voltage for constant current of 90 mA in Ar–H_2 and in pure Ar [16].

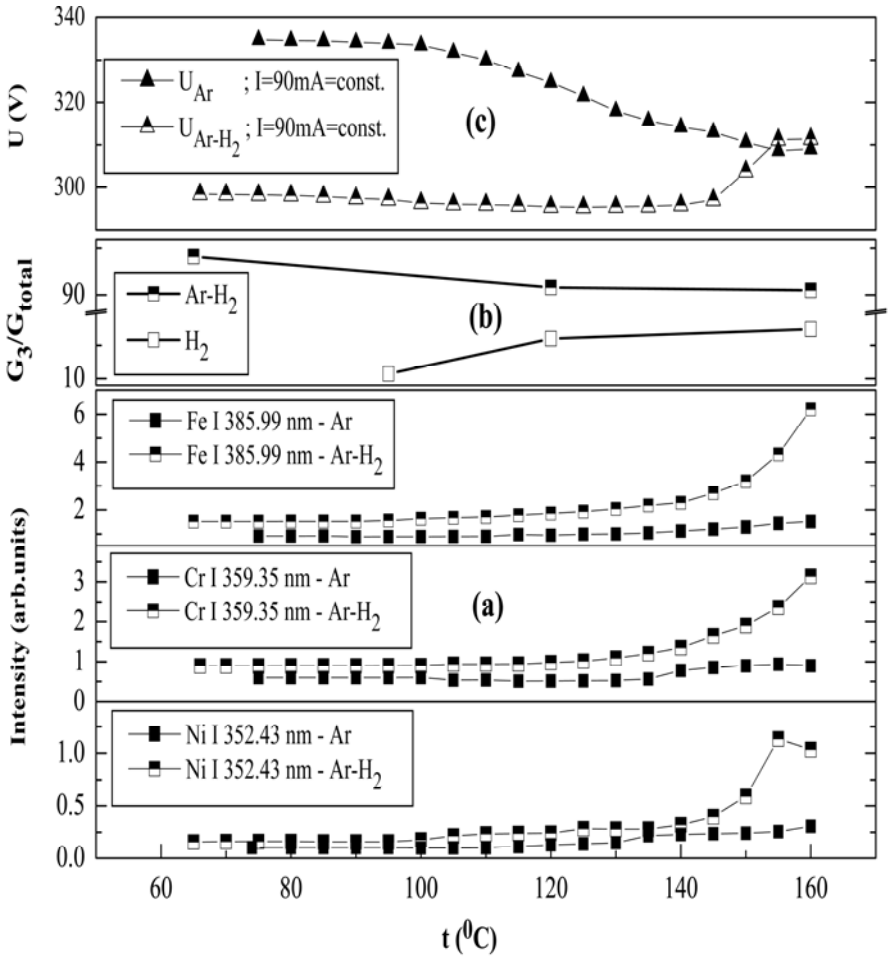

Fig. 7. The temperature dependence: of (a) Fe, Cr and Ni resonance lines intensity**;** (b) contribution of G_3/G_{total} to the H_α profile in H_2 and in Ar–H_2 **;** and (c) discharge voltage for constant current of 90 mA in Ar–H_2 and in pure Ar [16].

4. RADIAL DISTRIBUTION, INFLUENCE OF SURFACE COVERAGE AND TEMPERATURE EFFECT

The experiment in Ref. 16 was carried out using HC discharges observed end-on without attempting to achieve spatial resolution of the EDB of the Balmer lines. Our

recent study [28] is an extension of earlier ones [13,16], but with an emphasis on the radial distribution of the EDB of the H_α line in HC discharge in H_2 and Ar-H_2 mixtures.

The details of the HC discharge source are described earlier, see also [13]. The only difference is the cathode – anode distance, which was on one side 20 mm, and 15 mm on the other. In this way the discharge voltage can be changed using one or the other anode. During the discharge operation, the cathode was either air cooled with a fan, placed 150 mm from the discharge tube, or gradually heated by changing the cooling rate of the fan. The temperature of the outer wall of the HC tube is measured by a K-type thermocouple. The radial distribution spectra recordings were performed with unity magnification in equidistant steps perpendicular to the discharge axis, with an estimated spatial resolution of 0.25 mm or 0.40 mm. For radial intensity measurements the discharge was run between HC and rear anode, located at 20 mm from the cathode.

Three H_α line profiles recorded at various radial positions from the axis of HCGD operated with SS cathode in H_2 are presented in Figure 8a. In the upper right corner of this figure the experimental H_α profile recorded at the radial position *r=2.8 mm* and the best fit with three Gaussians are presented. The experimental conditions, relative contributions G_i/G_{total} (i=1,2,3) and energies E_i (i=1,2,3) of excited hydrogen atoms obtained by fitting the H□ profiles from titanium HC disharges are given in Tables 1 and 2.

An experimental study of the excessively broadened part G_3 of the Balmer alpha line in HCGD operated with H_2 and Ar-H_2 gas mixture with SS or Ti cathodes shows considerably different radial distribution depending upon the choice of operating gas. The differences between radial G_3 distribution with SS and Ti cathode are evident, see Figs. 9 and 10, and an increase with the HC temperature is always detected, see Tables 1 and 2.

With both HC operated in pure H_2, the radial distribution of the G_3 component is flat and therefore the overall profile has a bell shape, see Figures 9a and 10a. In order to explain the difference between G_3 contributions for HCGD with SS and Ti cathodes, the number R_N and the energy R_E coefficients for incident H^+ ions are calculated first for clean metal surface and than for surfaces covered with metal hydride layers. For this purpose we have utilized a FORTRAN subroutine [29] which implements a code described by Tabata and Ito [30]. This is not the only process of interaction between energetic particles and the cathode surface. The fast hydrogen atoms H_f, resulting from collisions of fast H^+ and H_3^+ ions with H_2, are also back scattered from the cathode surface. To analyze this process the results of a simulation with Fe and Ti targets using the binary collision cascade program MARLOWE [24] are used. Both sets of results for R_N and R_E, calculated and [24], show that the fraction of particles and energy reflected decreases with increasing hydrogen content of the metal hydride. Furthermore, both scattering coefficients are larger for Fe (very close to SS) than for Ti, see also Table 5 in Ref. 28 and [24]. For this reason the energy of excited hydrogen atoms (half-width of G_3 inenergy units) is larger for SS (E_3=*59 eV*) than for Ti HC (E_3=*50 eV*), in spite of similar voltage for both discharges. Thus, the results of both simulations, from Table 5 in Ref. 28 and [24], for Fe or SS and for Ti are in qualitative agreement with G_3 values

(proportional to R_N and R_E) and their temperature trend in Tables 1 and 2. The increase of G_3 contribution versus temperature may be related to the decrease of the metal hydride layer with an increase of HC temperature.

The secondary emission processes, which can affect the sheath field profile, and consequently the ion acceleration, are neglected in our analysis of discharge-surface interaction. This is due to the lack of secondary emission coefficients data for SS and Ti surfaces covered with a hydride layer having variable hydrogen/metal ratio.

At least, but not last, it is interesting to notice that similar line shapes of the H_α and D_α lines, see Figure 8a and [21], are detected close to the first wall and in plasma diverters of large plasma fusion devices, see e.g. [33-36] and references therein. Although in these cases Doppler broadening is combined with the Zeeman line splitting, the same elementary atomic and molecular collisions and interaction with the wall surface are also present. Therefore, the shape of the Balmer lines in high temperature plasma reactors must bear certain resemblance to those reported here. On the other hand, simple devices like HCGD may be used for material testing and for study of elementary processes relevant for large plasma devices.

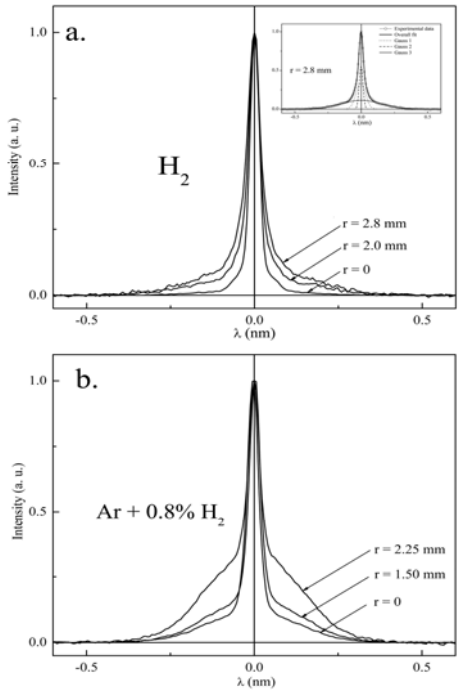

Fig. 8. Typical H_α profiles recorded at different radial positions in: (a) stainless steel hollow cathode; upper right corner depicts the H_α line shape at radial position *r=2.8 mm* fitted with three Gaussians; and (b) titanium hollow cathode. Discharge conditions: (a) pure H_2 at *p=4 mbar; I=90 mA; U=427V* and $T_{wall}=74^OC$; (b) Ar-H_2 mixture at *p=4 mbar; I=90 mA; U=338V* and $T_{wall}=75^OC$ [28].

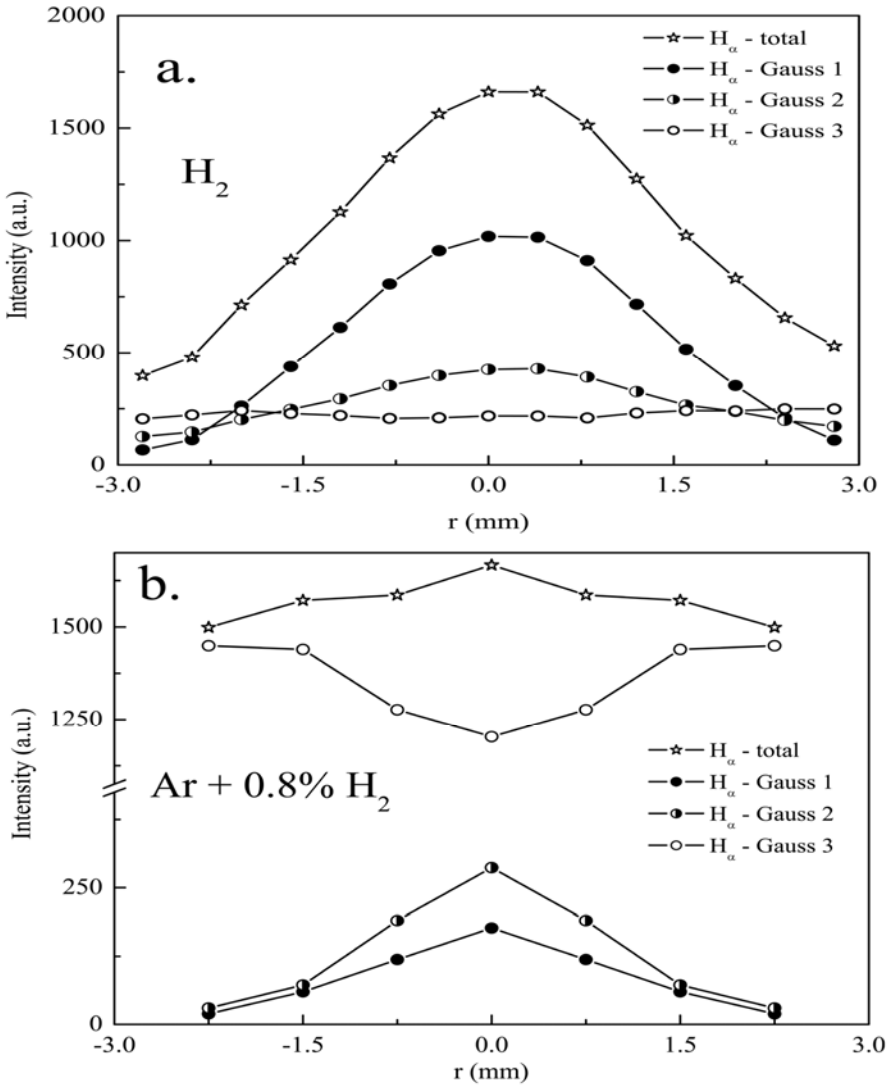

Fig. 9. The intensity distribution of the H_α spectral line and its Gaussian components vs. radial coordinate *r*. Experimental conditions: stainless steel hollow cathode discharge in (a) pure H_2 at *p=4 mbar; I=90 mA; U=427V* and $T_{wall}=74^OC$; (b) Ar-H_2 mixture at *p=4 mbar; I=90 mA; U=300V* and $T_{wall}=55^OC$ [28].

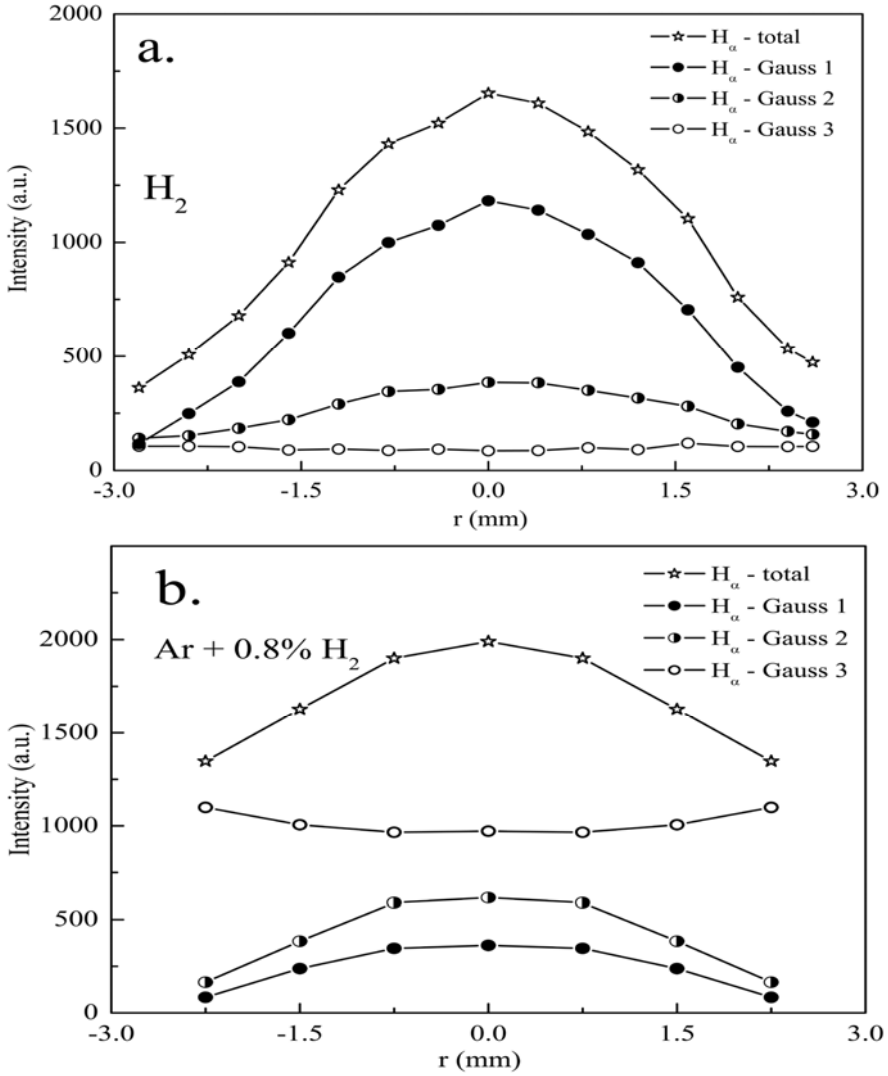

Fig. 10. The intensity distribution of the H□ spectral line and its Gaussian components vs. radial coordinate. Experimental conditions: titanium hollow cathode discharge in (a) pure H_2 at *p=4 mbar; I=90 mA; U=424V* and $T_{wall}=75^{O}C$; (b) Ar-H_2 mixture at *p=4 mbar; I=90 mA; U=338V* and $T_{wall}=75^{O}C$ [28].

Table 1. Experimental conditions, relative contributions G_i/G_{total} ($i=1,2,3$) and energies E_i ($i=1,2,3$) of excited hydrogen atoms obtained by applying three Gaussian fit to the $H_\square$ profiles for titanium hollow cathode glow discharge in pure H_2 at *p=4 mbar; I=90 mA*; *r* denotes radial position. [28]

T. (°C)	Voltage (V)	r (mm)	G_1/G_{total} (%)	G_2/G_{total} (%)	G_3/G_{total} (%)	Hydrogen Atom Energy		
						E_1 (eV)	E_2 (eV)	E_3 (eV)
74	424	0	71.4	22.3	6.3	0.3	5	50
		0.75	65.4	23.7	10.9		4	
		1.50	48.4	29.6	21.9			
		2.25	33.6	38.9	27.5		3	
100	435	0	66.5	25.3	8.2	0.3	5	
		0.75	59.8	27.0	13.2		4	
		1.50	39.6	35.8	24.6			
		2.25	20.9	42.9	36.2		3	
125	448	0	65.7	25.2	9.1	0.3	5	
		0.75	59.5	27.6	12.9		4	
		1.50	42.0	34.0	24.0			
		2.25	19.3	44.7	36.0		3	

Table 2. Same as for Table 1, but for glow discharge in argon-hydrogen mixture at *p=4 mbar; I=90mA*. [28]

T. (°C)	Voltage (V)	r (mm)	G_1/G_{total} (%)	G_2/G_{total} (%)	G_3/G_{total} (%)	Hydrogen Atom Energy		
						E_1 (eV)	E_2 (eV)	E_3 (eV)
75	338	0	19.0	31.0	51.0	0.3	1	37
		0.75	18.2	31.0	50.8			
		1.50	14.6	23.6	61.8			
		2.25	6.2	12.2	81.6			
100	336	0	14.8	28.7	56.5			
		0.75	16.9	26.7	56.4			
		1.50	10.5	18.2	71.3			
		2.25	4.9	8.5	86.6			
135	340	0	15.1	20.0	64.9			
		0.75	12.1	21.9	65.9			
		1.50	8.9	13.9	77.1			
		2.25	4.4	6.8	88.9			

ACKNOWLEDGMENT

This work within the Project 141029B "Low-temperature plasmas and gas discharges: radiative properties and interaction with surfaces» is supported by the Ministry of Science and Environmental Protection of the Republic of Serbia.

REFENECES

1. W. Benesh and E. Li, Opt. Lett. **9**, 338 (1984).
2. E. Li Ayers and W.Benesh, Phys. Rev. A **37**, 194 (1988).
3. M.R. Gemišić Adamov, B.M. Obradović, M.M. Kuraica and N. Konjević, IEEE Trans.Plasma Sci. **31**, 444 (2003).
4. M.R. Gemišić Adamov, M.M. Kuraica and N. Konjević, Eur.Phys.J. D **29**, 393 (2004).
5. N. Konjević and M. M. Kuraica, in The Physics of Ionized Gases, Eds: Lj. Hadžievski, T. Grozdanov, and N. Bibić, 22nd Summer School and International Symposium on the Physics of Ionized Gases, August 23 - 27, 2004, National Park Tara - Bajina Bašta, AIP Conference Proceedings 740 (2004) 268-281.
6. N. Cvetanović, M.M. Kuraica, N. Konjević, J.Apppl.Phys. **97**, 033302 (2005).
7. Z.Lj. Petrović, B.M. Jelenković, A.V. Phelps, Phys.Rev.Lett. **68**, 326 (1992).
8. S.B. Radovanov, K. Dzierzerga, J.R. Roberts, J.K. Ollthoff, Appl.Phys.Lett. **66**, 2637 (1995).
9. I.R. Videnović, N. Konjević, M.M. Kuraica, Spectrochim.Acta **51B**, 1707 (1996).
10. M. Kuraica and N. Konjević, Phys. Rev. A **46**, 4479 (1992).
11. M. Kuraica, N. Konjević, M. Platiša and D. Pantelić, Spectrochim. Acta **47B**, 1173 (1992).
12. M. Kuraica and N. Konjević, Phys. Scripta **50**, 487 (1994).
13. N.M. Šišović, G.Lj. Majstorović and N. Konjević, Eur. Phys. J. D **32**, 347–354 (2005).
14. R.L. Mills, P.C. Ray, B. Dandapani, R.M. Mayo, J. He, J.Appl.Phys.. **92**, 7008 (2002).
15. R.L. Mills, P.C. Ray, M. Nansteel, X. Chen, R.M. Mayo, J. He, B.Dandapapanii, IEEE Trans. Plasma. Sci. **31**, 338 (2003).
16. N. Konjević, G.Lj. Majstorović, N.M. Šišović, Appl.Phys.Lett. **86**, 251502 (2005).
17. B.P.Lavrov, A.S.Mel'nikov, Optics and Spectroscopy **75**, 1152 (1993).
18. T. Tabata, R. Ito, Y. Itikawa, N. Itoh, K. Morita, At. Data Nucl. Data Tables **31**, 1 (1984).
19. B.P.Lavrov, A.S.Mel'nikov, Optics and Spectroscopy **79**, 922 (1995).
20. A.V. Phelps, J.Appl.Phys. **98**, 066108 (2005).
21. NotesOnMills.pdf may be requested from avp@jila.colorado.edu
22. J. Roth, Chap.7 in Sputtering by Particle Bombardment II: Topics in Applied

Physics (Berisch, R., ed.) Vol.52, Springer-Verlag, Berlin (1983).
23. W. Eckstein and H. Verbeck, J.Nucl.Mat. **76&77**, 365 (1978).
24. O.S. Oen and M. T. Robinson, J.Nucl.Mat. **76&77**, 370 (1978).
25. J. Rooth, W. Eckstein and J. Bohdansky, J.Radiat.Eff. **48**, 231 (1980).
26. C. V. Budtz- Jorgensen, P. Kringhoj and J. Bottiger, Surf.Coat.Technol. **116-119**, 938 (1999).
27. J. Bohdansky, Nuclear Fusion, Special Issue, Data Compendium for Plasma Surface Interactions (1984) p.61.
28. N.M. Šišović, G.Lj. Majstorović and N. Konjević, Eur. Phys. J. D, accepted for publication.
29. M. Warrier, R. Schneider, X. Bonnin, Computer Phys.Comm. **160**, 46 (2004).
30. T. Tabata, R. Ito, Present status of data compilation on ion backscattering, Institute of Plasma Physics Report, Nagoya, Japan, IPPJ-AM-64:84–89, 1989.
31. A.V.Phelps, J.Phys.Chem.Ref.Data **19**, 653 (1990).
32. A.V.Phelps, J.Phys.Chem.Ref.Data **21**, 883 (1992).
33. J.D. Hey, C.C. Chu, E. Hintz, Contrib. Plasma Phys. **40,** 9 (2000).
34. M. Koubiti, Y. Marandet, A. Escarguel, H. Capes, L. Godbert-Mouret,R. Stamm, C. De Michelis, R. Guirlet, M. Mattioli, Plasma Phys.Control.Fusion **44,** 261 (2002).
35. J. D. Hey, C. C. Chu, Ph. Mertens, S. Brezinsek, B. Unterberg, J.Phys.B: At.Mol.Opt.Phys. **37**, 2543 (2004).
36. J. D. Hey, C C Chu, Ph. Mertens, J.Phys.B: At.Mol.Opt.Phys. **38**, 3517 (2005).